Yan *et al.*
Chinese Journal of Mechanical Engineering (2023) 36:53
https://doi.org/10.1186/s10033-023-00864-y

Chinese Journal of Mechanical Engineering

ORIGINAL ARTICLE

Open Access

Study of the Judder Characteristics of Friction Material for an Automobile Clutch and Test Verification

Zhengfeng Yan[1], Hangsheng Li[1], Hairui Lei[2], Maoqing Xie[3,4*] and Leigang Wang[3*]

Abstract

The friction judder characteristics during clutch engagement have a significant influence on the NVH of a driveline. In this research, the judder characteristics of automobile clutch friction materials and experimental verification are studied. First, considering the stick-slip phenomenon in the clutch engagement process, a detailed 9-degrees-of-freedom (DOF) model including the body, each cylinder of the engine, clutch and friction lining, torsional damper, transmission and other driveline parts is established, and the calculation formula of friction torque in the clutch engagement process is determined. Second, the influence of the friction gradient characteristics on the amplification or attenuation of the automobile friction judder is analyzed, and the corresponding stability analysis and the numerical simulation of different friction gradient values are carried out with MATLAB/Simulink software. Finally, judder bench test equipment and a corresponding damping test program are developed, and the relationship between the friction coefficient gradient characteristics and the system damping is analyzed. After a large number of tests, the evaluation basis of the test is determined. The research results show that the friction lining with negative gradient characteristics of the friction coefficient will have a judder signal. When the friction gradient value is less than −0.005 s/m, the judder signal of the measured clutch cannot be completely attenuated, and the judder phenomenon occurs. When the friction gradient is greater than − 0.005 s/m, the judder signal can be significantly suppressed and the system connection tends to be stable.

Keywords Clutch friction lining, Judder, Friction coefficient gradient, Damping, Bench test

1 Introduction

With the improvement of customers' requirements for automobile comfort, the vibration and noise problems of automobiles urgently need to be improved. As an important part of vehicle drivelines, clutches are widely used in various types of automobiles. In the process of starting and shifting, the self-excited vibration [1] caused by the friction between the driving and driven discs of a clutch will cause the judder of the clutch, which destroys the stability of the clutch engagement, reduces the ride comfort, intensifies the wear on the clutch, and reduces the service life of the clutch. Therefore, it is necessary to study the phenomenon of friction judder of the clutch. Based on a 2-DOF dynamic model, Bostwick et al. [2] proposed a modeling and simulation method for the clutch engagement judder process and qualitatively analyzed the friction judder mechanism. Crowther et al. [3, 4] developed a stick-slip algorithm to calculate the friction torque of the clutch and applied

*Correspondence:
Maoqing Xie
xiemaoqing@126.com
Leigang Wang
lgwang@ujs.edu.cn
[1] School of Automotive and Transportation Engineering, Hefei University of Technology, Hefei 230009, China
[2] Allways Friction Material (Kunshan) Co. Ltd, Suzhou 215332, China
[3] School of Materials Science & Engineering, Jiangsu University, Zhenjiang 212013, China
[4] Zhejiang Tieliu Clutch Co. Ltd., Hangzhou 311101, China

it to the powertrain with automatic transmission. The influence of applied pressure fluctuation of a clutch on the powertrain with or without automatic transmission was studied. Chen et al. [5] embedded the import damping model of a friction link into a 3-DOF dynamic model to study the judder mechanism from the perspective of friction import damping. Refs. [6, 7, 8, 9] established a 4-DOF model for a driveline, analyzed the mechanism and influencing factors of clutch friction judder in detail, and gave the corresponding improvement measures. Yang et al. [8] also added that the resistance torque excitation had the same effect on the friction judder as the pressure fluctuation. Zhang et al. [10] studied the relationship among modal coupling, the friction coefficient velocity slope, and the stick-slip motion. According to the symbols of the friction coefficient and the velocity slope, the unstable region of modal coupling was formed into four parts, and the influence of the four parts on the stick-slip motion was analyzed. Shangguan et al. [11, 12] studied the influence of the performance of the driven disc on vehicle judder and the car-shaking judder. It was found that increasing the static friction coefficient and reducing the moment of inertia of the driven disc and the second-stage torsional stiffness could reduce the joint judder and car-shaking judder of the vehicle during the starting process. Duan et al. [13] took a hydraulic torque converter as the research object, established a 3-DOF dynamic model, and analyzed the stick-slip characteristics during the connection of the hydraulic torque converter. Rahnejat et al. [14, 15, 16] established a torsional judder model with 7-DOF, calculated and analyzed the relationship between the friction coefficient and the relative velocity, and studied the influences of the relevant parameters of the driveline on the clutch judder. Based on the judder mechanism of a clutch, Gkinis and Paygude et al. [17, 18] analyzed the influences of the temperature and the pressure on the friction lining from the point of view of the friction lining material, and they determined the judder performance of different friction linings. Gregor et al. [19, 20] studied the performance of friction lining with different resin contents in a judder test based on multivariate statistical analysis and the torque signals of an actual bench test. Li et al. [21] examined the judder behavior of a centrifugal clutch from the start of hot spots in the conformal contact, then the repeated developments of thermoelastic instability, and finally the formation of cyclic undulations in the vibrations, friction coefficient, and torque. Yuan et al. [22, 23, 24] explored the mechanism of the vehicle start-up judder that seriously deteriorates ride comfort and then proposed a mechanism-oriented control strategy to cut off the introduction process of negative damping caused by the Stribeck effect for suppressing the vehicle start-up judder. The core idea of the mechanism-oriented control strategy is to cut off the positive-feedback closed loop, which is achieved by fine-tuning the position of the release bearing and finally the judder-suppression performance behaves well both in simulation and in the experiment. Hao et al. [25] used an uncertain hybrid model with random and interval variables to describe the uncertainty of parameters and a hybrid perturbation vertex method is formulated to compute the uncertainty. Furthermore, parameters with high sensitivities are used as design variables, and uncertainty-based optimization is conducted to reduce clutch judder.

Although previous scholars have conducted research on vehicle friction judder from different perspectives and studied the self-excited vibration caused by the friction between the driving and driven discs of a clutch and the relationship between the friction coefficient velocity slope and the stick-slip motion. However, the stability analysis of the friction coefficient gradient of the clutch friction material and its relationship with friction lining damping needs more detailed research. It is also a topic worthy of further study for testing bench and evaluation methods of the judder characteristics of clutch friction materials. Based on the previous research, the paper refines the dynamic model of the transmission system and further studies the mechanism of the friction judder. At the same time, according to the existing technical conditions, a judder testing bench and a standard experimental evaluation system were established to verify the judder characteristics. Firstly, this paper establishes a 9-DOF model, improves the accuracy of the mathematical model, and solves the calculation formula of friction torque in a stick-slip condition. Second, the influence of the friction coefficient gradient on the friction judder is analyzed, and the corresponding stability and simulation analysis is carried out. Finally, a special judder test bench and the corresponding damping test program are developed. Through theoretical analysis, the relevant test standards are formulated, and the test evaluation basis is established. The influence of the friction coefficient gradient on the amplification or attenuation of the friction judder signal is verified.

In this paper, the stability analysis of the friction coefficient gradient of the clutch friction material and its relationship with friction lining damping are studied in detail. A judder testing bench and evaluation method for the judder characteristics of clutch friction materials are proposed. The ideas and experimental evaluation basis provided in this paper can significantly improve the judder phenomenon during clutch engagement.

2 Clutch Engagement Dynamics Analysis and Modeling

2.1 Clutch Engagement Dynamics Model

Clutch engagement occurs in the starting and shifting process of a vehicle. It is a process in which the driving and driven parts begin to come into and produce relative sliding, and the speed of the driving and driven parts reaches a consistent sliding stop. In this process, judder often occurs. In order to study the phenomenon during the clutch engagement, we model the clutch in the driveline in detail based on the multiple degrees of freedom models established by previous researchers on this problem [26, 27, 28, 29]. We establish a 9-DOF dynamic model including the body, each cylinder of the engine, clutch and friction lining, torsional damper, transmission and other driveline parts based on the driveline structure shown in Figure 1. In the process of clutch engagement, there are two conditions stick and slip between the driving and driven parts of the clutch. When the driving part and the driven part of the clutch are in the slipping condition, the dynamic model is shown in Figure 2.

Based on the dynamic model shown in Figure 2, Eq. (1) is derived from the Lagrange equation:

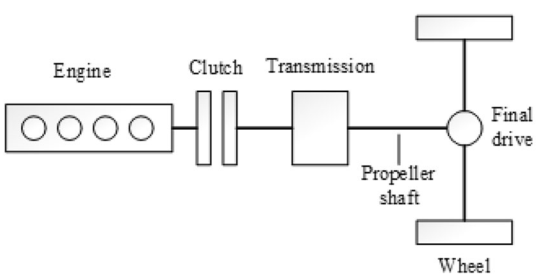

Figure 1 Structural diagram of driveline

$$\begin{cases} J_1\ddot{\theta}_1 + c_1\dot{\theta}_1 + k_1(\theta_1-\theta_2) = T_1, \\ J_2\ddot{\theta}_2 + c_2\dot{\theta}_2 - k_1(\theta_1-\theta_2) = -k_2(\theta_2-\theta_3), \\ J_3\ddot{\theta}_3 + c_3\dot{\theta}_3 - k_2(\theta_2-\theta_3) = -k_3(\theta_3-\theta_4), \\ J_4\ddot{\theta}_4 + c_4\dot{\theta}_4 + k_4(\theta_4-\theta_5) = k_3(\theta_3-\theta_4), \\ J_5\ddot{\theta}_5 + c_5\dot{\theta}_5 - k_4(\theta_4-\theta_5) = -T_2, \\ J_6\ddot{\theta}_6 + c_6\dot{\theta}_6 + k_5(\theta_6-\theta_7) = T_2, \\ J_7\ddot{\theta}_7 + c_7\dot{\theta}_7 + k_6(\theta_7-\theta_8) = k_5(\theta_6-\theta_7), \\ J_8\ddot{\theta}_8 + c_8\dot{\theta}_8 + k_7(\theta_8-\theta_9) = k_6(\theta_7-\theta_8), \\ J_9\ddot{\theta}_9 + c_9\dot{\theta}_9 - k_7(\theta_8-\theta_9) = -T_0, \end{cases} \tag{1}$$

where, J_1 is the equivalent moment of inertia of the crank connecting rod group of the first cylinder of the engine; J_2 is the equivalent moment of inertia of the crank connecting rod group of the second cylinder of the engine; J_3 is the equivalent moment of inertia of the crank connecting rod group of the third cylinder of the engine; J_4 is the equivalent moment of inertia of the crank connecting rod group of the fourth cylinder of the engine; J_5 is the equivalent moment of inertia of the flywheel and clutch driving part; J_6 is the equivalent moment of inertia of the friction lining and wave plate; J_7 is the equivalent moment of inertia of the torsional damper; J_8 is the equivalent moment of inertia of the transmission; J_9 is the equivalent moment of inertia of the body and other driveline components; $\theta_1, \theta_2, \theta_3, \theta_4, \theta_5, \theta_6, \theta_7, \theta_8, \theta_9$ are the rotation angles of the corresponding components; T_1 is the engine excitation torque, and T_2 is the friction torque transmitted between the driving part and the friction lining. T_0 is the equivalent resistance moment from the road resistance moment to the torsional damper; $c_1, c_2, c_3, c_4, c_5, c_6, c_7, c_8$ and c_9 are the equivalent viscous damping coefficients of each part; k_1, k_2, k_3, k_4 are the equivalent torsional stiffness of the crank journal of each cylinder of the engine; k_5, k_6 and k_7 are the the spring stiffness of the torsional damper, the equivalent torsional stiffness of the transmission input shaft and the

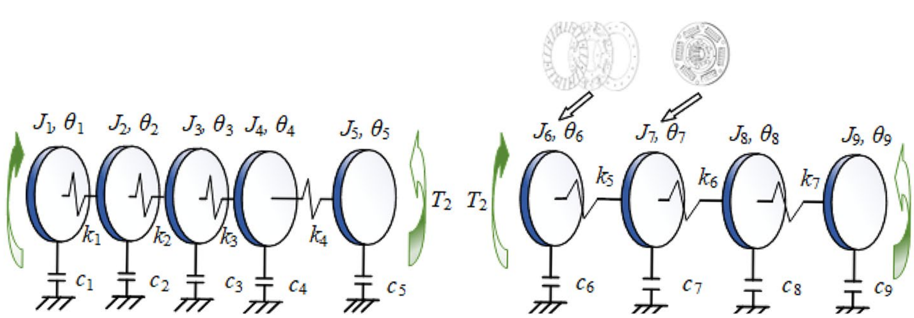

Figure 2 Dynamic model in slipping condition

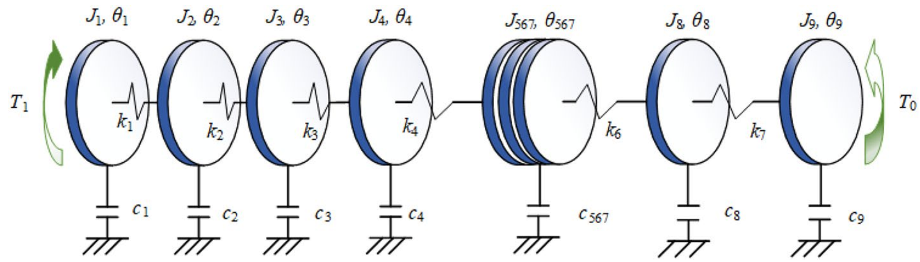

Figure 3 Dynamic model in sticking condition

equivalent torsional stiffness of the transmission output shaft, respectively.

When the clutch driving and driven parts are in the sticking condition, the dynamic model is as shown in Figure 3.

In Figure 3, J_{567}, c_{567}, and θ_{567} are the equivalent rotational inertia, equivalent damping coefficient, and angular displacement of the clutch, respectively, and the remaining parameters are constant. The dynamics equations in the sticking condition are expressed as shown in Eq. (2):

$$\begin{cases} J_1\ddot{\theta}_1 + c_1\dot{\theta}_1 + k_1(\theta_1-\theta_2) = T_1, \\ J_2\ddot{\theta}_2 + c_2\dot{\theta}_2 - k_1(\theta_1-\theta_2) = -k_2(\theta_2-\theta_3), \\ J_3\ddot{\theta}_3 + c_3\dot{\theta}_3 - k_2(\theta_2-\theta_3) = -k_3(\theta_3-\theta_4), \\ J_4\ddot{\theta}_4 + c_4\dot{\theta}_4 + k_4(\theta_4-\theta_{567}) = k_3(\theta_3-\theta_4), \\ J_{567}\ddot{\theta}_{567} + c_{567}\dot{\theta}_{567} - k_4(\theta_4-\theta_{567}) = -k_6(\theta_{567}-\theta_8), \\ J_8\ddot{\theta}_8 + c_8\dot{\theta}_8 + k_7(\theta_8-\theta_9) = k_6(\theta_{567}-\theta_8), \\ J_9\ddot{\theta}_9 + c_9\dot{\theta}_9 - k_7(\theta_8-\theta_9) = -T_0, \end{cases} \tag{2}$$

where $J_{567} = J_5 + J_6 + J_7$, $c_{567} = c_5 + c_6 + c_7$, $\theta_{567} = \theta_5 = \theta_6 = \theta_7$.

2.2 Friction Torque of Clutch Under Stick-slip Condition

In the process of clutch engagement, there is friction torque between the driving and driven parts and the calculation of friction torque needs to consider many factors [30]. There are sticking and sliding phenomena in the clutch engagement process, and the friction torque in the two conditions is not the same. When the clutch is slipping, the friction torque is expressed as shown in Eq. (3):

$$T_2 = n\mu R_{\mathrm{m}} F, \tag{3}$$

where F is the pressing force acting on the surface of the friction lining; R_m is the equivalent friction radius of the clutch; μ is the sliding friction coefficient, and n is the number of friction surfaces. The calculation formula of the equivalent friction radius is expressed as shown in Eq. (4):

$$R_{\mathrm{m}} = \frac{2(R_0^3 - R_{\mathrm{i}}^3)}{3(R_0^2 - R_{\mathrm{i}}^2)}, \tag{4}$$

where R_0 is the outer radius of the friction lining, and R_{i} is the inner radius of the friction lining.

According to the classical Coulomb friction law [31, 32], the magnitude of friction is independent of the velocity, but practice shows that the actual friction coefficient is not a constant value, but rather a function of the relative velocity [33]. Most studies define the two with nonlinear relationships. In order to facilitate analysis, the relationship between the friction coefficient and the relative velocity of the clutch tested in this study is approximately linear. Ignoring the influence of pressure and temperature on the friction coefficient, there is a relationship between the friction coefficient and the relative sliding velocity of the clutch which is expressed as shown in Eq. (5):

$$\mu = \mu_0 + \mu'(\dot{\theta}_5 - \dot{\theta}_6), \tag{5}$$

where μ' is the friction coefficient gradient; μ_0 is the static friction coefficient, and $\dot{\theta}_5 - \dot{\theta}_6$ is the velocity difference between the driving part and the friction lining. Substituting Eq. (5) into Eq. (3), the friction torque calculation Eq. (6) for the slipping condition is obtained.

$$T_2 = n\mu_0 R_{\mathrm{m}} F + \mu'(\dot{\theta}_5 - \dot{\theta}_6) n R_{\mathrm{m}} F. \tag{6}$$

When the clutch is in the sticking condition, the friction torque transmitted by the clutch is:

$$T_2 = \begin{cases} T_{\mathrm{full}}, & \dot{\theta}_5 - \dot{\theta}_6 = 0, |T_{\mathrm{full}}| \le T_{\max}, \\ \mathrm{sgn}(T_{\mathrm{full}})T_{\max}, & \dot{\theta}_5 - \dot{\theta}_6 = 0, |T_{\mathrm{full}}| > T_{\max}, \end{cases} \tag{7}$$

where, $T_{\max}$ is the maximum static friction torque; T_{full} is the torque transmitted when the clutch is fully engaged, and the force analysis of the driving part and the friction lining can be carried out separately, as shown in Eqs. (8) and (9):

$$T_{\mathrm{full}} = -J_5 \ddot{\theta}_5 - c_5 \dot{\theta}_5 + k_4(\theta_4 - \theta_5), \tag{8}$$

(Analysis of the driving part)

$$T_{\mathrm{full}} = J_6 \ddot{\theta}_6 + c_6 \dot{\theta}_6 + k_5(\theta_6 - \theta_7). \tag{9}$$

(Analysis of the friction lining)

In summary, the friction torque of the clutch in the two conditions of sticking and slipping can be expressed as shown in Eq. (10):

$$T_2 = \begin{cases} n\mu_0 R_{\mathrm{m}} F + \mu^{'}(\dot{\theta}_5 - \dot{\theta}_6) n R_{\mathrm{m}} F, & \dot{\theta}_5 - \dot{\theta}_6 \neq 0, \\ T_{\mathrm{full}}, & \dot{\theta}_5 - \dot{\theta}_6 = 0, |T_{\mathrm{full}}| \leq T_{\max}, \\ \mathrm{sgn}(T_{\mathrm{full}}) T_{\max}, & \dot{\theta}_5 - \dot{\theta}_6 = 0, |T_{\mathrm{full}}| > T_{\max}. \end{cases} \tag{10}$$

3 Effect of Friction Coefficient Gradient on Judder Characteristic

Frictional judder is caused by the change of the friction coefficient relative to the sliding velocity, which may occur in any system that transmits force or torque through friction. The sensitivity of the system to friction judder is defined by the friction coefficient gradient, which is defined as the change of the friction coefficient μ relative to the sliding speed v or ω, the expression is shown in Eq. (11). According to the existing research and analysis, the friction coefficient gradient is considered to have three situations: positive gradient, zero gradient and negative gradient. The changes of the three friction coefficient gradients are shown in Figure 4.

$$\mu^{'} = \frac{\mathrm{d}\mu}{\mathrm{d}\triangle v}, \tag{11}$$

where Δv denotes the speed difference between the driving part and the driven part.

According to the dynamic model of Figure 2, the dynamic equation can be written as:

$$T_2 = J_6 \ddot{\theta}_6 + c_6 \dot{\theta}_6 + k_5(\theta_6 - \theta_7). \tag{12}$$

Substituting Eq. (6) into Eq. (12):

$$n\mu_0 R_{\mathrm{m}} F + \mu^{'}(\dot{\theta}_5 - \dot{\theta}_6) n R_{\mathrm{m}} F = J_6 \ddot{\theta}_6 + c_6 \dot{\theta}_6 + k_5(\theta_6 - \theta_7). \tag{13}$$

Finishing Eq. (13):

$$(\mu_0 + \mu^{'} \dot{\theta}_5) n R_{\mathrm{m}} F = J_6 \ddot{\theta}_6 + (c_6 + \mu^{'} n R_{\mathrm{m}} F) \dot{\theta}_6 + k_5(\theta_6 - \theta_7). \tag{14}$$

The solution of the homogeneous equation corresponding to Eq. (14) is:

$$\theta_6 = e^{\alpha t}[\sqrt{C_1^2 + C_2^2} \cos(\beta t - \phi)]. \tag{15}$$

In Eq. (15):

$$\alpha = \frac{c_6 + \mu^{'} n R_{\mathrm{m}} F}{2J_6}, \tag{16}$$

$$\beta = \frac{\sqrt{(c_6 + \mu^{'} n R_{\mathrm{m}} F)^2 - 4J_6 k_5}}{2J_6}, \tag{17}$$

$$\phi = \arctan \frac{C_2}{C_1}, \tag{18}$$

where, C_1, C_2 are arbitrary constants, while C_1 is not 0.

The amplitude of the system is $e^{\alpha t}\sqrt{C_1^2 + C_2^2}$. Therefore, when $\mu' \geq 0$, $\alpha \leq 0$ and $e^{\alpha t} < 1$, the amplitude of the system attenuates, the judder disappears, and the system tends to be stable. When $\mu' < 0$, the friction coefficient decreases with the increasing sliding speed, at this time, $\alpha \geq 0$, $e^{\alpha t} > 1$, the amplitude of the system increases, the judder is strengthened, and the system is in an unstable state.

4 Gradient Stability Analysis of Clutch Friction Coefficient

For the dynamic model of the clutch engagement process established in Sect. 2.1, it can be seen from the analysis in Sect. 2.2 that only Eq. (1) needs to be analyzed in the calculation process. Eq. (1) can be written as the following matrix form [3, 17, 34]:

$$\boldsymbol{J}\ddot{\boldsymbol{\theta}} + \boldsymbol{C}\dot{\boldsymbol{\theta}} + \boldsymbol{K}\boldsymbol{\theta} = \boldsymbol{T}. \tag{19}$$

In Eq. (19),

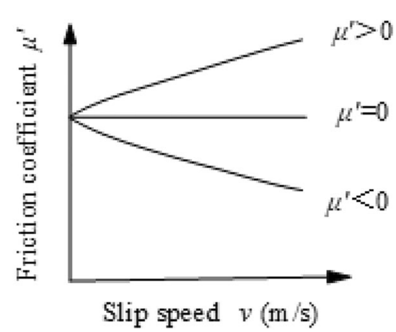

Figure 4 Defined as the gradient of the friction coefficient

$$\boldsymbol{J}=\begin{pmatrix} J_1 &&&&&&&& \\ & J_2 &&&&&&& \\ && J_3 &&&&&& \\ &&& J_4 &&&&& \\ &&&& J_5 &&&& \\ &&&&& J_6 &&& \\ &&&&&& J_7 && \\ &&&&&&& J_8 & \\ &&&&&&&& J_9 \end{pmatrix}, \tag{20}$$

$$\boldsymbol{C}=\begin{pmatrix} c_1 &&&&&&&& \\ & c_2 &&&&&&& \\ && c_3 &&&&&& \\ &&& c_4 &&&&& \\ &&&& c_5+\mu' nR_{\mathrm{m}}F & -\mu' nR_{\mathrm{m}}F &&& \\ &&&& -\mu' nR_{\mathrm{m}}F & c_6+\mu' nR_{\mathrm{m}}F &&& \\ &&&&&& c_7 && \\ &&&&&&& c_8 & \\ &&&&&&&& c_9 \end{pmatrix}, \tag{21}$$

$$\boldsymbol{K}=\begin{pmatrix} k_1 & -k_1 &&&&&&& \\ -k_1 & k_1+k_2 & -k_2 &&&&&& \\ & -k_2 & k_2+k_3 & -k_3 &&&&& \\ && -k_3 & k_3+k_4 & -k_4 &&&& \\ &&& -k_4 & k_4 &&&& \\ &&&&& k_5 & -k_5 && \\ &&&&& -k_5 & k_5+k_6 & -k_6 & \\ &&&&&& -k_6 & k_6+k_7 & -k_7 \\ &&&&&&& -k_7 & k_7 \end{pmatrix}, \tag{22}$$

$$\boldsymbol{T}=\begin{pmatrix} T_1 \\ 0 \\ 0 \\ 0 \\ -\mu_0 nR_{\mathrm{m}}F \\ \mu_0 nR_{\mathrm{m}}F \\ 0 \\ 0 \\ -T_0 \end{pmatrix}. \tag{23}$$

In order to facilitate the numerical calculation, the dynamic Eq. (19) can be written as the initial value problem of differential equations :

$$\begin{cases} \boldsymbol{X}=\boldsymbol{A}\dot{\boldsymbol{X}}+\boldsymbol{BU}, \\ \boldsymbol{X}(0)=\boldsymbol{X}_0, \end{cases} \tag{24}$$

where, $\boldsymbol{X}=\left(\theta_1\ \theta_2\ \theta_3\ \theta_4\ \theta_5\ \theta_6\ \theta_7\ \theta_8\ \theta_9\ \dot{\theta}_1\ \dot{\theta}_2\ \dot{\theta}_3\ \dot{\theta}_4\ \dot{\theta}_5\ \dot{\theta}_6\ \dot{\theta}_7\ \dot{\theta}_8\ \dot{\theta}_9\right)^{\mathrm{T}}$ is the state vector, and $\boldsymbol{A}=\begin{pmatrix} \boldsymbol{0} & \boldsymbol{I} \\ -\boldsymbol{J}^{-1}\boldsymbol{K} & -\boldsymbol{J}^{-1}\boldsymbol{C} \end{pmatrix}$ is the Jacobi matrix of the system, $\boldsymbol{B}=\begin{pmatrix} \boldsymbol{0} \\ \boldsymbol{J}^{-1} \end{pmatrix}$, $\boldsymbol{U}=\boldsymbol{T}$.

Based on the Lyapunov stability theory, the eigenvalues of the Jacobian matrix $\boldsymbol{A}$ can be used as the basis for the stability determination for linear time-invariant systems. If the real parts of all of the eigenvalues of the Jacobian matrix $\boldsymbol{A}$ are less than 0, the system is stable, and its natural response will eventually approach equilibrium. If the maximum real part of all eigenvalues is equal to 0, the system is critically stable, but as long as there is an eigenvalue whose real part is greater than 0, the system will lose stability.

The moment of inertia, stiffness, damping and engine excitation parameters in the model are shown in Table 1. The actual vehicle is a damped system, but when analyzing the influence of the friction coefficient on the stability, the presupposed system is undamped; that is, $c_1, c_2, c_3, c_4, c_5 c_6, c_7, c_8$ and c_9 are all zero. The clutch static friction coefficient μ_0 is set to 0.3. In order to maintain the consistency of the theoretical analysis and the experiment, μ' is selected as the four parameter values of −0.01 s/m, −0.005 s/m, 0 s/m, 0.005 s/m, which are input into the state matrix $\boldsymbol{A}$. The eigenvalue of each μ' is obtained. The selection of the friction coefficient gradient value can be found in Ref. [1]. The results are shown in Table 2.

According to the calculation results, when the friction coefficient gradient is negative, the real part of the system eigenvalue appears to have a positive value, the system produces judder behavior, and the system loses stability. The smaller the friction coefficient gradient value is, the more unstable the system is. When the friction coefficient gradient is 0, the real part of the matrix eigenvalue is 0, and the system is in a critical stable state; when the friction coefficient is positive, the real part of the eigenvalues of the system matrix does not appear to have positive value, and the system is in a stable state.

5 Simulation Analysis of Clutch Friction Coefficient Gradient

Based on MATLAB / Simulink software, the gradient values of the friction coefficient are selected as − 0.01 s/m, − 0.005 s/m, 0 s/m and 0.005 s/m for the simulation. The simulation results are shown in Figure 5.

Table 1 Parameters of a vehicle

Variable	Implication	Value
$J_1(\mathrm{kg}\cdot\mathrm{m}^2)$	Equivalent moment of inertia of the crank connecting rod group of the first cylinder of the engine	0.0182
$J_2(\mathrm{kg}\cdot\mathrm{m}^2)$	Equivalent moment of inertia of the crank connecting rod group of the second cylinder of the engine	0.0182
$J_3(\mathrm{kg}\cdot\mathrm{m}^2)$	Equivalent moment of inertia of the crank connecting rod group of the third cylinder of the engine	0.0182
$J_4(\mathrm{kg}\cdot\mathrm{m}^2)$	Equivalent moment of inertia of the crank connecting rod group of the fourth cylinder of the engine	0.0182
$J_5(\mathrm{kg}\cdot\mathrm{m}^2)$	Inertia of flywheel and driving part of clutch	0.5
$J_6(\mathrm{kg}\cdot\mathrm{m}^2)$	Equivalent moment of inertia of friction lining and wave plate	0.015
$J_7(\mathrm{kg}\cdot\mathrm{m}^2)$	Equivalent rotational inertia of clutch driven disc hub	0.04
$J_8(\mathrm{kg}\cdot\mathrm{m}^2)$	Equivalent rotational inertia of transmission	0.02
$J_9(\mathrm{kg}\cdot\mathrm{m}^2)$	Equivalent moment of inertia of body and other driveline components	4
$c_1(\mathrm{Nms}\cdot\mathrm{rad}^{-1})$	The damping of the crank journal of the first cylinder of the engine	0
$c_2(\mathrm{Nms}\cdot\mathrm{rad}^{-1})$	The damping of the crank journal of the second cylinder of the engine	0
$c_3(\mathrm{Nms}\cdot\mathrm{rad}^{-1})$	The damping of the crank journal of the third cylinder of the engine	0
$c_4(\mathrm{Nms}\cdot\mathrm{rad}^{-1})$	The damping of the crank journal of the fourth cylinder of the engine	0
$c_5(\mathrm{Nms}\cdot\mathrm{rad}^{-1})$	Equivalent damping of flywheel and clutch driving part	0
$c_6(\mathrm{Nms}\cdot\mathrm{rad}^{-1})$	Friction lining damping	0
$c_7(\mathrm{Nms}\cdot\mathrm{rad}^{-1})$	Torsional damper damping	0
$c_8(\mathrm{Nms}\cdot\mathrm{rad}^{-1})$	Transmission equivalent damping	0
$c_9(\mathrm{Nms}\cdot\mathrm{rad}^{-1})$	Equivalent damping of body and other driveline components	0
$k_1(\mathrm{Nm}\cdot\mathrm{rad}^{-1})$	Equivalent torsional stiffness of the crank journal of the first cylinder of the engine	20000
$k_2(\mathrm{Nm}\cdot\mathrm{rad}^{-1})$	Equivalent torsional stiffness of the crank journal of the second cylinder of the engine	20000
$k_3(\mathrm{Nm}\cdot\mathrm{rad}^{-1})$	Equivalent torsional stiffness of the crank journal of the third cylinder of the engine	20000
$k_4(\mathrm{Nm}\cdot\mathrm{rad}^{-1})$	Equivalent torsional stiffness of the crank journal of the fourth cylinder of the engine	20000
$k_5(\mathrm{Nm}\cdot\mathrm{rad}^{-1})$	Spring equivalent stiffness of torsional damper	2000
$k_6(\mathrm{Nm}\cdot\mathrm{rad}^{-1})$	Equivalent torsional stiffness of transmission input shaft	4000
$k_7(\mathrm{Nm}\cdot\mathrm{rad}^{-1})$	Equivalent torsional stiffness of transmission output shaft	6000
$T_1(\mathrm{N}\cdot\mathrm{m})$	Engine excitation torque	300
$T_0(\mathrm{N}\cdot\mathrm{m})$	Road resistance torque	100
$F(\mathrm{N})$	Clutch pressure	4000
$R_0(\mathrm{m})$	Outer radius of friction lining	0.2
$R_i(\mathrm{m})$	Inner radius of friction lining	0.134
μ_0	Static friction coefficient	0.3

According to the simulation results, when the friction coefficient gradient is negative, the system has a strong judder phenomenon. Specifically, when the friction gradient is − 0.01 s/m, the judder signal is significantly amplified. When the gradient value is nonnegative, the oscillation of the system is improved and the oscillation signal of the system is convergent. According to the comprehensive comparison, the theoretical analysis and simulation results are in good agreement.

6 Bench Test of Judder Characteristics of Friction Lining

6.1 Experimental Equipment

The experimental equipment is shown in Figures 6 and 7. The motor in the drive unit is used as the power source, and the torque is transmitted to the clutch at different speeds. The control cylinder achieves the separation and connection of the clutch by separating the fork. In the process of clutch connection, the torsional data are transmitted to the data collector by the speed sensor installed on the spline shaft holder. The driven disc is mounted on the spline shaft connected to the damping torsion bar, and the torque is transmitted to the torsion bar. One end of the torsion bar is

Table 2 Stability analysis results of different friction coefficient gradients

μ'	Real part	Imaginary part
− 0.01	0.0000	±1.6562*i*
	0.2144	±1.0688*i*
	0.0001	±0.9246*i*
	0.0210	±0.7424*i*
	0.0329	±0.3220*i*
	0.0041	±0.0983*i*
	0.0678	±0.0319*i*
	0.0038	±0.0046*i*
	0.0000	±0.0000i
− 0.005	0.0002	±0.4772*i*
	0.0025	±0.3864*i*
	0.4665	±0.32391*i*
	0.0747	±0.5961*i*
	0.3405	±0.7428*i*
	0.1464	±0.1666*i*
	0.0047	±0.0950*i*
	0.1662	±0.9247*i*
	0.0018	±0.0000*i*
0	0.0000	±1.3572*i*
	0.0000	±1.8790*i*
	0.0000	±1.4684*i*
	0.0000	±0.9248*i*
	0.0000	±0.7433*i*
	0.0000	±0.4408*i*
	0.0000	±0.1948*i*
	0.0000	±0
	0.0000	±0
0.005	-0.0012	±0.0000*i*
	-0.0025	±0.1971*i*
	-0.0001	±0.1608*i*
	-0.0210	±0.1055*i*
	-0.0329	±0.0742*i*
	-0.1464	±0.0387*i*
	-0.4465	±0.0319*i*
	0.0000	±0.0046*i*
	0.0000	±0.0000*i*

fixed, so the torque transmitted makes the torsion bar torsional. Because the clutch is not fully connected, the clutch fails to completely transmit the torque to the torsion bar, so the torsion bar swings. With full contact between the clutch disc and the pressure disc and the flywheel, the clutch friction lining does not judder, and the torsion bar stops at a specific angle and halts the torsion pendulum.

6.2 Experimental Method

The clutch judder test is performed using an ALLWAYS test bench. The motor power is 45 kW, and test procedures refer to the internal standards of the 3102 test procedures. First, the weight of the whole cover assembly and the flywheel is determined, the clamping thickness of the driven disc is measured for the clamping load, and the weight of the driven disc is determined. In the second step, three cycles are tested (150 applications reach 15 kJ), followed by cooling at 800 r/min for two hours. The above steps are repeated, and 37, 40, 80 cycles are performed (corresponding to 1850, 2000, 4000 applications) until 20000 applications are performed. At the end of the test, additional judder tests are carried out at 200 °C and 250 °C. Finally, the clamping thickness of the driven disc is measured for the clamping load, and the weight of the driven disc is determined. The weight of the friction lining is also measured.

6.3 Test Program

In order to obtain the damping value of the clutch friction lining at different times, the mechanism for obtaining the damping value of the friction lining is analyzed. Based on the free vibration excitation of the single-DOF system [35], the friction lining is taken as the research object, and a theoretical analysis is applied to the longitudinal dynamics of the vehicle. The vibration time displacement curve is shown in Figure 8.

The solution of Eq. (12) consists of the solution of the corresponding homogeneous equation and the solution of the non-homogeneous equation. Letting

$$2\sigma = \frac{c_6}{J_6}, \tag{25}$$

$$\omega_0^2 = \frac{k_5}{J_6}, \tag{26}$$

where σ is the damping coefficient and ω_0 is the inherent angular frequency of the system, and the corresponding homogeneous equation is:

$$\theta_6 + 2\sigma\,\dot{\theta}_6 + \omega_0^2\theta_6 = 0. \tag{27}$$

Eq. (27) is solved to obtain Eq. (28):

$$\theta_6 = Ae^{-\sigma t}\cos\left(\sqrt{\omega_0^2 - \sigma^2}t + \phi\right), \tag{28}$$

where A denotes the maximum amplitude of the system, ϕ is the phase angle, t is time and the ratio of two adjacent amplitudes A_1 and A_2 is called the attenuation coefficient d:

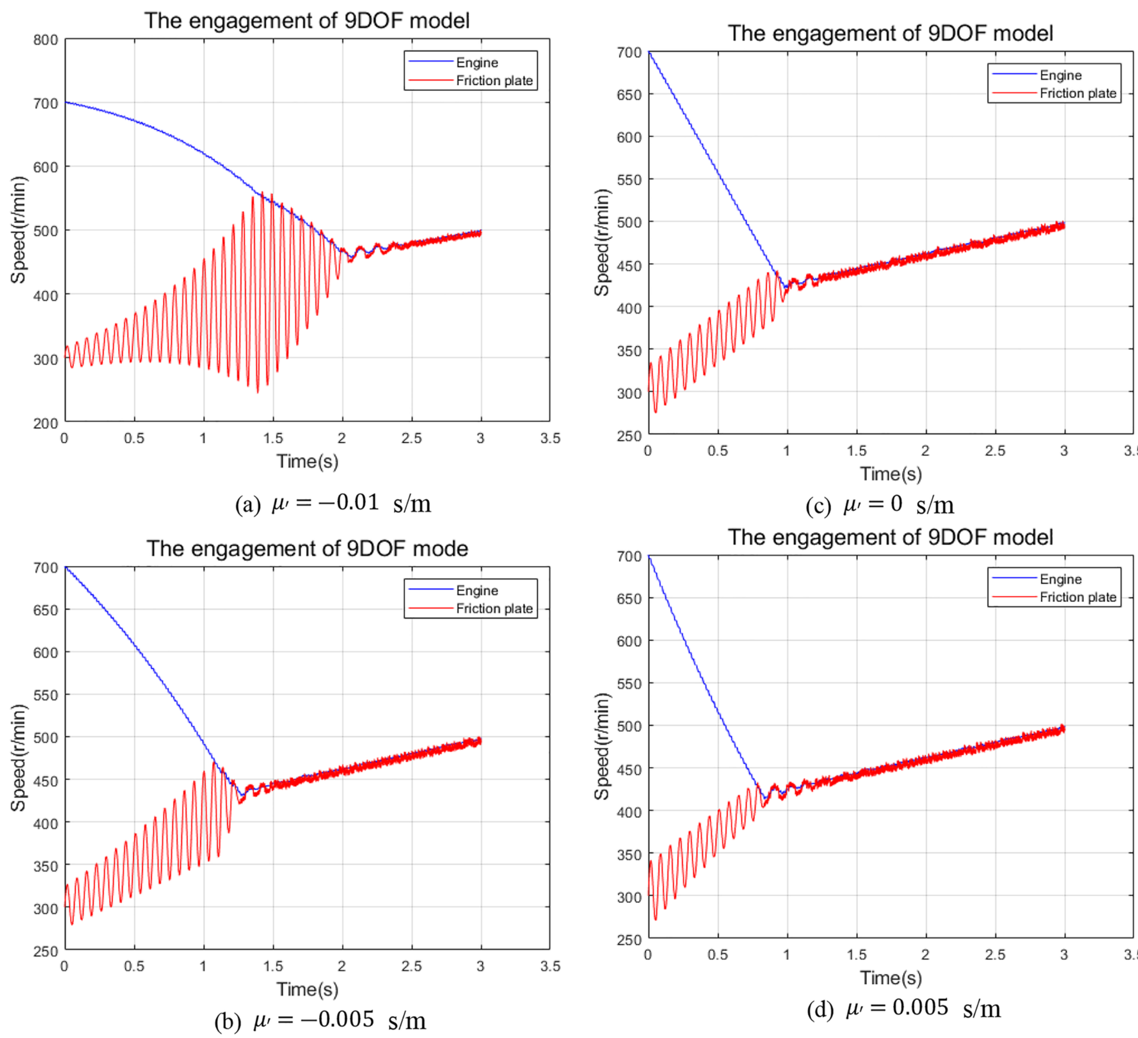

Figure 5 Simulation diagrams for different friction gradients (**a**) $\mu' = -0.01$ s/m (**b**) $\mu' = -0.005$ s/m (**c**) $\mu' = 0$ s/m (**d**) $\mu' = 0.005$ s/m

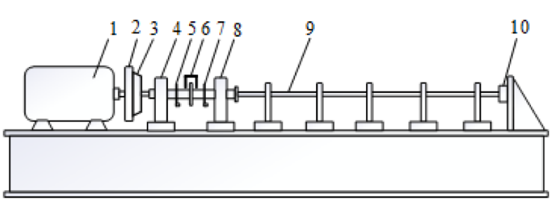

1 Driving unit, 2 Rotational speed, contact force, friction surface temperature sensor, 3 Clutch, 4 Bearing seat, 5 Torsional damper, 6 Additional damper, 7 Angle acceleration (receiver), 8 Bearing seat, 9 Torsion bar, 10 Torque measurement shaft

Figure 6 Judder test bench

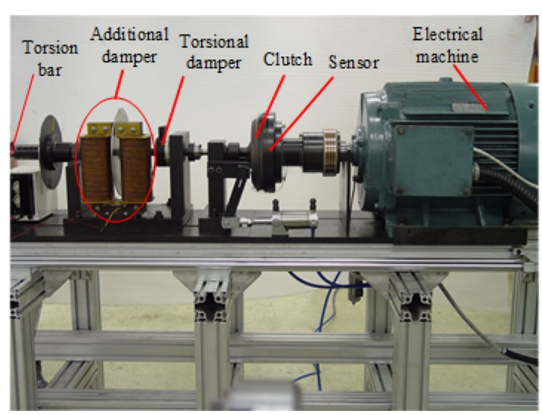

Figure 7 Actual diagram of judder test bench

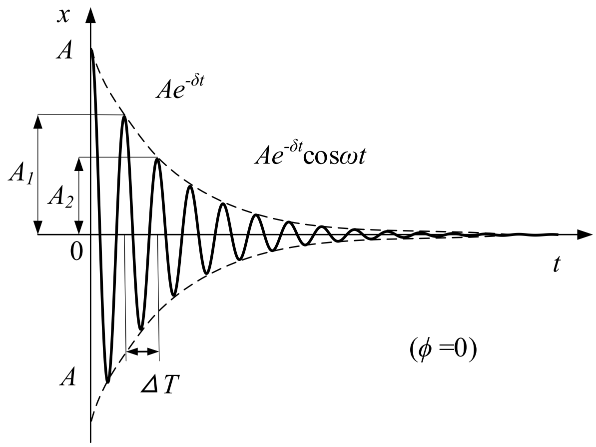

Figure 8 Damping vibration displacement time curve

$$d=\frac{A_1}{A_2}=\frac{Ae^{-\sigma t}}{Ae^{-\sigma(t+\Delta T)}}=e^{\sigma\Delta T}, \tag{29}$$

where ΔT is the time difference. Taking the logarithms on both sides of Eq. (29) at the same time:

$$\ln\frac{A_1}{A_2}=\sigma\Delta T. \tag{30}$$

Converting Eq. (30) into a velocity expression:

$$\ln\frac{Speed_1}{Speed_2}=\sigma\Delta T. \tag{31}$$

According to Eqs. (25) and (31), the calculation formula of the principle of the test program can be obtained as follows:

$$c_6=2J_6\ln\frac{Speed_1}{Speed_2}\times\frac{1}{\Delta T}. \tag{32}$$

According to Eq. (32), based on the above analysis and principle derivation, a judder test program is developed to obtain the damping value of the friction lining at different times. The program calculates the damping value for the current condition according to the point we choose. The program interface is shown in Figure 9.

6.4 Evaluation Basis

For vehicle friction judder, subjective evaluation and objective evaluation are generally adopted. Subjective evaluation is based on the feelings of drivers and passengers in the process of vehicle starting, while objective evaluation is based on the measured damping coefficient of the friction lining and the damping value set on the bench. Taking the friction lining as the research object, based on the viscous damping model, Eq. (33) is obtained as:

$$T_2=-c_6\,\dot{\theta}_6, \tag{33}$$

where simultaneous derivation of $\dot{\theta}_6$ is performed on both sides.

$$\frac{\mathrm{d}T_2}{\mathrm{d}\dot{\theta}_6}=-c_6. \tag{34}$$

In the Coulomb friction zone, the derivative of $\dot{\theta}_6$ on both sides of Eq. (3) is obtained as follows:

$$\begin{aligned}\frac{\mathrm{d}T_2}{\mathrm{d}\,\theta_6}&=\frac{\mathrm{d}(n\mu R_\mathrm{m}F)}{\mathrm{d}\,\theta_6}=nR_\mathrm{m}F\frac{\mathrm{d}\mu}{\mathrm{d}\,\theta_6}\\&=nR_\mathrm{m}F\frac{\mathrm{d}\mu}{\mathrm{d}v}\cdot\frac{\mathrm{d}v}{\mathrm{d}\,\theta_6}=nR_\mathrm{m}^2F\frac{\mathrm{d}\mu}{\mathrm{d}v}\\&=n\mu' R_\mathrm{m}^2F.\end{aligned} \tag{35}$$

The simultaneous Eqs. (34) and (35) are solved, and the Eq. (36) is obtained as follows:

$$c_6+n\mu' R_\mathrm{m}^2F=0. \tag{36}$$

In this test example, the clutch friction lining of the Luk company with a diameter of 200 mm and a pressing force of 1500 N is used. Its number is 32411 R/3.5 (ϕ200 mm$\times\phi$134 mm$\times$ 3.5 mm), and the number of contact surfaces of the friction lining is $n=2$. The equivalent friction radius of the friction lining is 85.2 mm, and the critical friction coefficient gradient when the system judders is $\mu'=-0.005$ [1]. The general automotive powertrain damping is considered to be 0.1 Nms [36], and the additional dampers are used to simulate the damping of the vehicle powertrain, and attenuate the judder signal caused by the friction lining self-excited vibration. According to Eq. (36), the set value c_{add} of the additional damper in the bench device is as shown in Eq. (37):

$$c_\mathrm{add}=-n\mu' R_\mathrm{m}^2F=0.1\mathrm{Nms}. \tag{37}$$

6.5 Test Result

When the system damping is greater than 0.1 Nms due to the self-excited vibration of the friction lining, the damping value set by the additional damper cannot completely suppress the judder signal, and the system will produce judder behavior. When the system damping is less than 0.1 Nms due to self-excited vibration of the friction lining, the additional damper attenuates the judder signal and the system tends to be stable. The test results of the damping value caused by the self-excited vibration of the friction lining shown in Figure 9 are

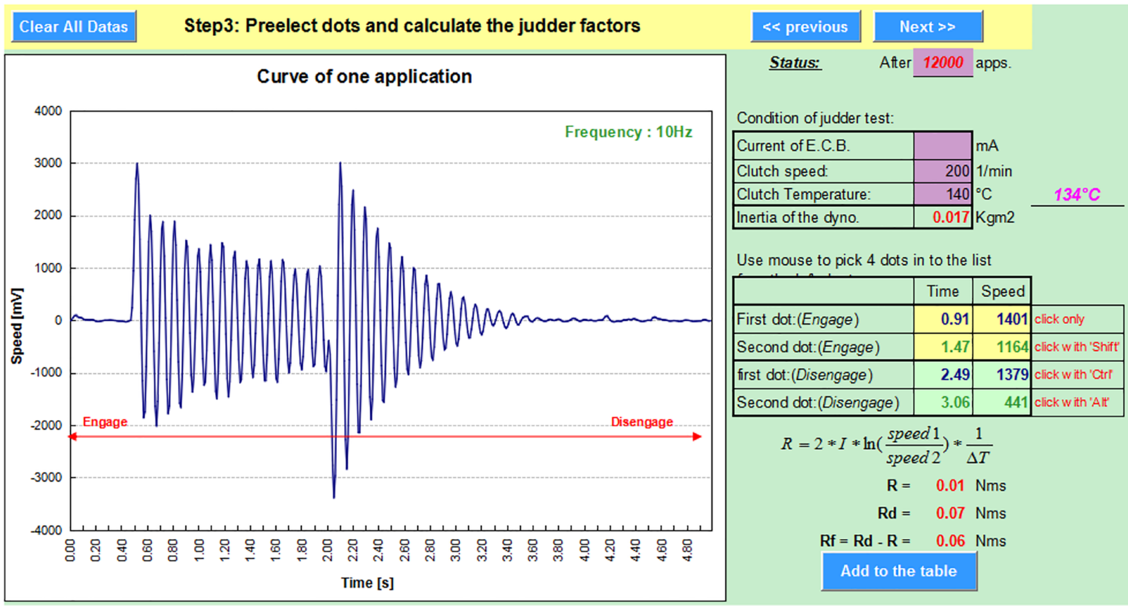

Figure 9 Test program interface

0.06 Nms, which is less than 0.1 Nms. The judder signal is attenuated by the additional damper, and the system tends to be stable, which has an inhibitory effect on the judder. Figure 10 shows the judder test reports under different friction coefficient gradients. Among them, the test results of the damping value of the friction lining due to self-excited vibration shown in Figure 10(a) are less than 0.1 Nms. The judder signal is attenuated by the additional damper, and the system tends to be stable, which has an inhibitory effect on judder. The test results of the damping value of the friction lining due to self-excited vibration shown in Figure 10(b) are greater than 0.1 Nms, and the system has a strong judder phenomenon, the judder is not suppressed.

7 Conclusions

With the dynamic analysis of an automobile driveline, a 9- DOF dynamic model is established. Taking the friction lining as the research object, the influence of the friction coefficient gradient on the automobile friction judder is analyzed, and then the influence of the self-excited vibration of the friction lining on the automobile friction judder is analyzed. Based on the analysis of a test bench, the following conclusions can be drawn:

(1) There are two conditions of sticking and slipping in the clutch engagement process. By analyzing the dynamic models of the two conditions, the calculation model of the friction torque in the clutch engagement process is determined.

(2) When the friction characteristic of the friction lining in the clutch has a negative gradient, the system loses stability and judder occurs; when the clutch friction characteristics have a zero gradient or a positive gradient, the system is in a stable state and the judder does not occur. Therefore, as far as possible, the friction gradient is chosen as a positive material to make the friction lining.

(3) Through theoretical and simulation analysis, it is determined that when the self-excited vibration of the clutch friction lining is too large and the system damping is not enough to attenuate the judder signal, the system loses stability. With the improvement of the friction gradient characteristics of the clutch friction material, the friction coefficient gradient value is greater than − 0.005 s/m, which can effectively reduce the degree of system judder.

(4) Based on the existing test standards and the viscous damping model of the single-DOF system, a clutch friction lining judder test bench and the corresponding damping test program are designed and developed. After a large number of tests, the experimental evaluation basis is established. Through the experimental analysis, it is concluded that the damping value set by the additional damper is 0.1 Nms. When the system damping caused by the self-excited vibration of the friction lining exceeds 0.1 Nms, the additional damper cannot completely

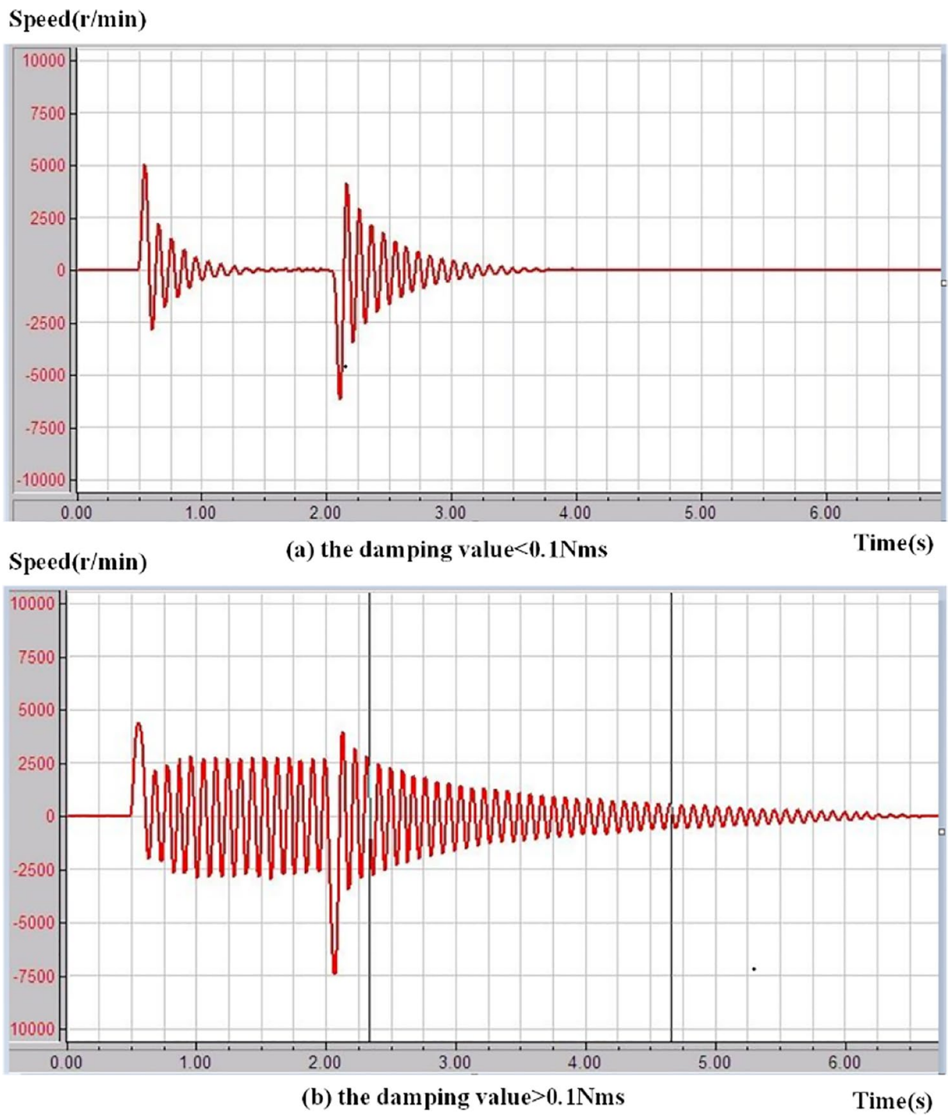

Figure 10 Test report

suppress the judder signal, and the system produces judder behavior. When the system damping caused by the self-excited vibration of the friction lining does not exceed 0.1 Nms, the additional damper attenuates the judder signal and the system tends to be stable.

Acknowledgements
Not applicable.

Author contributions
ZY is responsible for the structure of the whole article; HL is responsible for writing manuscripts, dynamic modeling and simulation analysis, and stability analysis; HL is responsible for experimental equipment development and experimental data analysis; MX is the corresponding author and is responsible for the analysis of the effect of friction coefficient gradient on judder characteristics; LW is the co-corresponding author and responsible for the proofreading and review of the paper. All authors read and approved the final manuscript.

Authors' Information
Zhengfeng Yan, born in 1969, is currently a professor at *Hefei University of Technology, China*. He received his B.Sc. degree in mechanical engineering from *Chongqing University*, *China*, in 1991, and the M.Sc. degree in industry engineering from *Huazhong University of Science and Technology, China*, in 2003, and the Ph.D. degree in mechanical manufacturing and automation from *Wuhan University of Technology, China*, in 2009. His research interests include automotive components design and manufacturing, advanced manufacturing technology, product development and design.
Hangsheng Li, born in 1996, is currently a master candidate at *School of Automotive and Transportation Engineering, Hefei University of Technology, China*.
Hairui Lei, born in 1981, is currently a technical director of *Allways Friction Materials (Kunshan) Co., Ltd., China*. His research interests include tribology, electromechanical engineering, etc.

Leigang Wang, born in 1963, is currently a doctoral supervisor at *School of Materials Science & Engineering, Jiangsu University, China*. His research interests include CAD/CAE/CAM of mold, plastic processing tribology, and material mechanics behavior computer simulation.

Maoqing Xie, born in 1974, is currently a professor-level senior engineer at *Zhejiang Tieliu Clutch Co., Ltd., China*. He received his Ph.D. degree at *School of Materials Science & Engineering, Jiangsu University, China.* His research interests include advanced manufacturing technology, new material technology, friction materials science and mold design and manufacturing.

Funding

Supported by National Natural Science Foundation of China (Grant No. 51775249).

Availability of data and materials

The datasets supporting the conclusions of this article are included within the article.

Declarations

Competing interests

The authors declare no competing financial interests.

Received: 25 January 2022 Revised: 18 October 2022 Accepted: 17 February 2023
Published online: 17 April 2023

References

[1] A Albers, D Herbst. Chatter-causes and solutions. *6th LUK Kolloquim*, 1998: 23-45.

[2] C C Bostwick, A Szadkowski. Self-excited vibrations during engagements of dry friction clutches. *SAE Technical Papers*, Indianapolis, Indiana, USA, November 16-18, 1998: 982846.

[3] A R Crowther, N Zhang, D K Liu, et al. Analysis and simulation of clutch engagement judder and stick-slip in automotive powertrain systems. *Proceedings of the Institution of Mechanical Engineers Part D: Journal of Automobile Engineering*, 2004, 218(12): 1427-1446.

[4] A R Crowther, N Zhang. Torsional finite elements and nonlinear numerical modelling in vehicle powertrain dynamics. *Journal of Sound & Vibration*, 2005, 284(3-5): 825-849.

[5] L Chen, H S Wang, G Xi. Clutch engagement control based on stability analysis. *Journal of System Simulation*, 2011, 23(7): 1451-1458. (in Chinese)

[6] H W Hu, X J Zhou, X Y Yang, et al. Analysis of clutch engagement judder and its influence factors. *Journal of Zhejiang University(Engineering Science)*, 2009, 43(3): 535-539. (in Chinese)

[7] S Y Jin, G Q Wu, L J Wang. Analysis and simulation on the shudder phenomena in automatic transmission vehicles. *Automotive Engineering*, 2013, 35(8): 701-705. (in Chinese)

[8] L K Yang, H Y Li, B Ma. Friction-induced vibration of wet clutches. *Journal of Vibration and Shock*, 2016, 35(9): 117-122. (in Chinese)

[9] L Yu, B Ma, II Y Kim, et al. Influences of the uneven contact pressure and the initial temperature on the hot judder behavior in a multi-disc clutch. *Proceedings of the Institution of Mechanical Engineers, Part J: Journal of Engineering Tribology*. 2019, 234(4): 500-514.

[10] L J Zhang, J Wu, D J Meng. Relationship among mode coupling, friction-velocity slope and stick- slip motion. *Journal of Tongji University: Natural Science*, 2015, 43(12): 1850-1859. (in Chinese)

[11] X L Liu, W B Shangguan, L Li, et al. Research for clutch disc parameters on the shuffle of vehicle at starting. *Journal of Vibration, Measurement & Diagnosis*, 2017, 37(6): 1127-1135. (in Chinese)

[12] W B Shangguan, T Sun, R Y Zheng, et al. Effect of the performance of the driven disc of the friction clutch on vehicle judder during starting. *Journal of Vibration Engineering*, 2016, 29(3): 488-497. (in Chinese)

[13] C W Duan, R Singh. Stick-slip behavior in torque converter clutch. *SAE Paper*, Traverse City, Michigan, USA, May 16-19, 2005: 2005-01-2456.

[14] D Centea, H Rahnejat, M T Menday. The influence of the interface coefficient of friction upon the propensity to judder in automotive clutches. *Proceedings of the Institution of Mechanical Engineers, Part D: Journal of Automobile Engineering*, 1999, 213(3): 245-258.

[15] D Centea, H Rahnejat, M T Menday. Non-linear multi-body dynamic analysis for the study of clutch torsional vibrations (judder). *Applied Mathematical Modelling*, 2001, 25(3): 177-192.

[16] M T Menday, H Rahnejat. Friction lining characteristics and the clutch take up judder phenomenon with manual transmission. *Tribology & Dynamics of Engine & Powertrain*, 2010: 680-702.

[17] T Gkinis, R Rahmani, H Rahnejat. Effect of clutch lining frictional characteristics on take-up judder. *Proceedings of the Institution of Mechanical Engineers Part K: Journal of Multi-body Dynamics*, 2017, 231(3): 493-503.

[18] T Paygude, R R Joshi. Modeling and analysis of clutch engagement judder in commercial vehicle powertrain systems. *WCX SAE World Congress Experience,* USA, April 2, 2019: 2019-01-0784.

[19] I R S Gregori, C E Thomaz, C G Martins. Multivariate judder behavior analysis of dry clutches based on torque signal and friction material. *2014 IEEE Vehicle Power and Propulsion Conference (VPPC),* Coimbra, Portugal, October 27-30, 2014: 14916084.

[20] I S Gregori, W H Jr. Judder based on sub scale test machine concerning facing. *SAE 2013 World Congress & Exhibition,* USA, April 08, 2013: 2013-01-1436.

[21] T C Li, Y W Huang, J F Lin. Studies on centrifugal clutch judder behavior and the design of frictional lining materials. *Mechanical Systems & Signal Processing*, 2016, 66-67: 811-828.

[22] R F Yuan, G Q Wu. Dynamic analysis of vehicle start-up judder based on elasto-plastic friction model and dry clutch maneuvering characteristic. *Proceedings of the Institution of Mechanical Engineers, Part K: Journal of Multi-body Dynamics*, 2019, 233(2): 455-469.

[23] R F Yuan, G Q Wu. Mechanism analysis of vehicle start-up judder based on gradient characteristic of Stribeck effect. *Proceedings of the Institution of Mechanical Engineers Part D: Journal of Automobile Engineering,* 2019, 234(2-3):1-17.

[24] R F Yuan, G Q Wu, C H Shao, et al. Mechanism-oriented control for suppressing start-up judder of vehicle with automatic dry clutch: Experiment and simulation analysis. *Proceedings of the Institution of Mechanical Engineers, Part D: Journal of Automobile Engineering*, 2021, 235(2-3): 744-758.

[25] Y D Hao, Z C He, G Y Li, et al. Analysis and optimization of clutch judder based on a hybrid uncertain model with random and interval variables. *Engineering Optimization*, 2018, 50(11): 1894-1913.

[26] S Y Lin. *Design and manufacturing of diaphragm spring and Belleville spring clutch*. Nanjing: Southeast University Press, 1995. (in Chinese)

[27] L P Li, Z J Lu, X L Liu, et al. Modeling and analysis of friction clutch at a driveline for suppressing car starting judder. *Journal of Sound and Vibration*, 2018, 424: 335-351.

[28] L K Yang, H Y Li, M Ahmadian, et al. Analysis of the influence of engine torque excitation on clutch judder. *Journal of Vibration and Control,* 2017, 23(4): 645-655.

[29] L H Li, R Singh. Analysis of start-up transient for a powertrain system with a nonlinear clutch damper. *Mechanical Systems & Signal Processing*, 2015, 62-63: 460-479.

[30] X H Lin, J Q Xi, S Q Hao. The calculation model of the friction torque on a dry clutch. *Proceedings of the Institution of Mechanical Engineers, Part D: Journal of Automobile Engineering*. 2017, 231(13): 1796-1805.

[31] L L Liu, H Z Liu, Z Y Wu, et al. An overview of friction models in mechanical systems. *Advances in Mechanics*, 2008, 38(2): 201-213. (in Chinese)

[32] D N Yuan, L L Liu, H Z Liu, et al. Progress of pre-sliding friction model. *Journal of System Simulation*, 2009, 21(4): 1142-1147. (in Chinese)

[33] S Z Wen. *Tribological principle*. Beijing: Tsinghua University Press, 1990. (in Chinese)

[34] F Yu, Y lin. *Automobile system dynamics*. Beijing: China Machine Press, 2005. (in Chinese)

[35] Y Wang, Y P Yang, J S Zhao. A study on dynamic properties of a forced oscillation system. *College Physics*, 2001, 20(7): 22-25. (in Chinese)

[36] I R S Gregori. Methodology to determine the clutch facing sensitivity regarding judder in the vehicle. *SAE Brasil International Noise and Vibration Congress*, USA, October 17-19, 2010: 2010-36-0501.